

Study on the Fatigue of a Spherical Bearing Under Different Loading Conditions Considering Rotation Effect

Yadi FU*, Hangyu WANG**, Yanqing FU***

*Beijing Construction Engineering Group Co., Ltd, Beijing, China

** China Agricultural University, Department. of Civil Engineering, Beijing, China

***Central Research Institute of Building and Construction Co., Ltd. MCC, China.

E-mail: 191607093@qq.com (Corresponding Author)

crossref <http://dx.doi.org/10.5755/j02.mech.31433>

1. Introduction

In recent years, with the rapid development of long-span spatial structure, the stress analysis of its structure is more and more strict. Joints are an important part of spatial structure and the key to the promotion of spatial structure [1-2]. Bearing is a kind of joint. As an important component connecting the superstructure and substructure, it can transfer the reaction force of the superstructure to the substructure, coordinate and release the deformation of the superstructure [3]. Besides, it is an important factor to realize the assumption of structural boundary and influence the stability bearing capacity of the structure [4]. Bearing forms mainly include plate bearing, rubber cushion bearing and spherical bearing, etc. In recent years, lead-core rubber bearing, high damping rubber bearing and other new energy-dissipating bearings have appeared [5-7]. The spherical bearing is a new kind of bearing developed on the basis of the basin type rubber bearing, which belongs to a kind of steel bearing. Due to the advantages of long service life, large bearing capacity, flexible rotation, suitable to large angle and large displacement of the beam end [8, 9], spherical bearings are widely used in highways, bridges and long-span structures [10, 11]. In recent years, because of its good machining performance, cast steel material is often used as a connector for joints with large stress and complex structure in spatial structures (especially special-shaped joints). In foreign countries, especially in developed countries such as Germany and Japan, cast steel joints have been widely used [12-14].

Spherical bearing joints in engineering structures are in a complex stress state, which is controlled by wind load and earthquake action in addition to gravity load and temperature action [15]. Under the action of earthquake and temperature, the bearing may sustain a lot of horizontal force, while under the action of wind load, the bearing may withstand great wind suction [7, 16, 17]. However, the traditional spherical bearing is designed to transfer vertical load, and its rotational capacity under the action of horizontal force is poor [10 – 13], and its resistance to drawing is poor under the action of tension. According to the disaster statistics of Wenchuan and Lushan earthquakes, bearing joints may fracture and fail during earthquakes due to the reciprocating effects of complex stresses such as bending, shear and tension [18]. And fatigue fracture is one of the main failure modes. Therefore, it is very important to study the mechanical properties of spherical bearing joints under static loads and the fatigue life under cyclic loads.

At present, there are few studies on the fatigue performance of spherical bearings. He [3] analyzed the fatigue life of a railway spherical bearings by finite element software ANSYS and fatigue software FEMFAT, and obtained the fatigue life of the bearings under actual working conditions. Liu [19] predicted and analyzed the service life of a light rail bearing by the combination of finite element simulation and test, and the results verified the rationality of the finite element method and the fatigue life of the bearing met the design requirements. He et al. [20] studied the fatigue temperature effect of a lead-core rubber bearing through cyclic loading test, and found that the temperature change caused by fatigue temperature effect of the bearing was proportional to the initial yield stress and inversely proportional to the bearing height. Tie [21] evaluated the service life of rubber and steel bearings of a bridge through finite element software ANSYS, and concluded that the recommended service life of rubber bearings is 50 years, and the steel bearings can work normally in their design life. In addition, Wu [18], Wang [22], Wang [23] et al. studied the fatigue of the anchor bolt of the bearing joints by means of tests. Thus, it can be seen that most research on the fatigue life of bearings is focused on railway and bridge bearings. The mainly studied bearings are rubber bearings, and most of them adopt the experimental research method, which has a long period, harsh test conditions and large cost. By using finite element software to simulate the fatigue performance of the bearing in working state, the reliability of the test can be verified, and a convenient method for fatigue life estimation of the bearing is provided.

In this paper, the finite element software ABAQUS will be used to study the static performance of a large cast steel spherical bearing, and on the basis, the fatigue life analysis of its each component will be mainly carried out by the fatigue software.

2. Basic structure of the spherical bearing

The traditional spherical bearing is composed of upper bearing plate (including stainless steel plate), planar PTFE plate, spherical PTFE plate and dustproof structure, etc. The sliding between the planar PTFE plate and the stainless-steel plate of the upper bearing plate can meet the displacement needs of the bearing, and the rotation function is realized by the sliding between the spherical crown liner plate and spherical PTFE plate [24].

Considering the requirements of the pull-out resistance and rotation performance of the bearing, based on the traditional spherical bearing, an improvement is

proposed in this paper. Four wedge-shaped parts are used to make the upper and lower bearing plates butt (as shown in Fig. 1), which effectively improves the pull-out ability of the bearing. At the same time, a rotation angle of $0\sim 3^\circ$ is allowed between the upper bearing plate and the ball core, and the rotational ability of the bearing is also improved, as shown in Fig. 2.



a) upper bearing plate b) ball core c) lower bearing plate

Fig. 1 Diagram of each part of the bearing

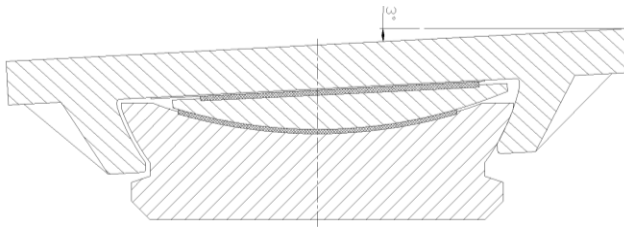


Fig. 2 Diagram of spherical bearing rotation angle

3. Static performance of the spherical bearing structure

3.1. Finite element model

3.1.1. Geometric dimensions and material properties

The spherical bearing 3D model was established in CAD and imported into ABAQUS for finite element analysis. The dimensions of each part of the bearing are shown in Fig. 3. The design basis of the spherical bearing is the Code for Seismic Design of Buildings (GB50011-2010) [25], Structural Design Standard (GB50017-2017) [26], Technical Code for Application of Cast Steel Joints (CECS 235:2008) [27] and Spherical Bearing for Building Steel Structure (GB/T32836-2016) [28].

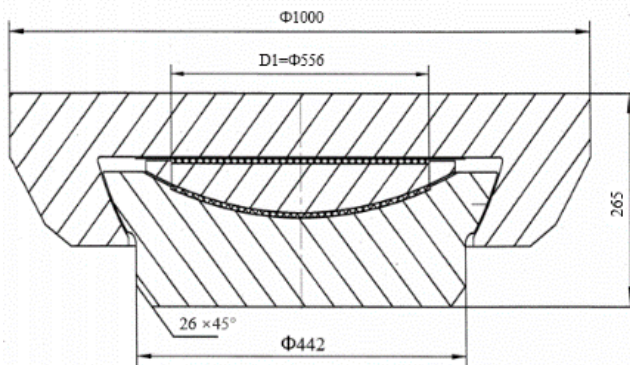


Fig. 3 Spherical bearing size

Cast steel G20Mn5QT is selected as the material for each part of the spherical bearing. The test results in the reference [29] are adopted as the mechanical property parameters. And the material constitutive relationship adopts the double broken line constitutive model, with elastic modulus $E = 2.17 \times 10^5$ MPa, yield strength $\sigma_s = 503.7$ MPa and ultimate strength $f_u = 624.5$ MPa. At the position where the

ball core is in contact with the upper and lower bearings, lubricating oil will be applied to reduce wear, and special wear resistant material will be added to solve the loosening compensation caused by wear.

3.1.2. Model building and unit division

The finite element model is established as shown in Fig. 4, with a total of 33,376 nodes. The contact part between the lower bearing plate and the upper bearing plate adopts C3D4 element, with a total of 8,320, and the other parts adopts C3D8R element, with a total of 25,472. The minimum element size is 3.6 mm, and the mesh division of the whole bearing is shown in Fig. 5.

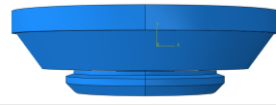


Fig. 4 Finite element model of the spherical bearing



Fig. 5 Meshing diagram

3.1.3. Contact and constraint settings

Considering that the upper bearing plate, the lower bearing plate and the ball core are not completely fixed in the actual working state, sliding and rotation are allowed. So the surface-to-surface contact method is adopted in ABAQUS to constrain it and simulate its actual working state [30]. The form of fixed constraint is adopted at the bottom of the lower bearing plate, and the vertical pressure, vertical tension and horizontal shear force are applied to the upper bearing plate in the form of surface load.

3.1.4. Load condition

According to the actual working state of the spherical bearing, the following four working conditions are determined.

1. Working condition 1: 3400 kN vertical pressure;
2. Working condition 2: 1000 kN vertical tension;
3. Working condition 3: 3400 kN vertical pressure and 800kN horizontal shear force in X or Z direction;
4. Working condition 4: 1000 kN vertical tension and 800 kN horizontal shear force in X or Z direction.

3.2. Results and analysis

Through modeling in the software of ABAQUS and define material, adding boundary conditions and loads, stress results of the bearing can be obtained under the above loads.

The maximum stress and its position of the bearing under the working conditions 1 and 2 are shown in Table 1.

It can be seen from Table 1 that, under the same vertical pressure, with the increase of the rotation angle of the upper bearing plate, the maximum stress of the bearing also gradually increases, and the position of which is at the ball core. Under the action of the same vertical tension, when the rotation angle of the upper bearing plate is 2° , the maximum stress of the bearing is the largest, and located at the lower bearing wedge-shape region.

Under the action of working condition 3, the maximum stress and its position of the bearing are shown in Table 2.

Table 1

Stress and position of the bearing under working conditions 1 and 2

Angle	Working condition	Vertical pressure		Vertical tension	
		The maximum stress /MPa	Location	The maximum stress /MPa	Location
0°		43.56	Ball core	445.5	Lower bearing wedge
1°		450.5		504.8	
2°		504.8		505	
3°		505		238.3	Upper bearing wedge

Table 2

Stress and position of the bearing under working condition 3

Angle	Working condition	Pressure and shear forces in the X direction		Pressure and shear forces in the Z direction	
		The maximum stress /MPa	Location	The maximum stress /MPa	Location
0°		513.4	Lower bearing wedge-shape	510.9	Lower bearing wedge-shape
1°		492.3	Ball core	511.7	
2°		492		517.5	
3°		487.9		522.5	

As can be seen from Table 2, under the same combined action of vertical pressure and X-direction shear force, the maximum stress of the bearing gradually decreases with the increase of the rotation angle of the upper bearing plate, and the position of the maximum stress of the bearing mostly occurs at the ball core. Under the combined action of the same vertical pressure and the Z-direction shear force,

the maximum stress of the bearing increases with the increase of the rotation angle of the upper bearing plate, and the position of the maximum stress of the bearing is all the wedge-shaped part of the lower bearing.

Under the action of working condition 4, the maximum stress and its position of the bearing are shown in Table 3

Table 3

Stress and position of the bearing under working condition 4

Angle	Working condition	Tension and shear force in the X direction		Tension and shear force in the Z direction	
		The maximum stress /MPa	Location	The maximum stress /MPa	Location
0°		433.5	Upper bearing wedge-shape	435.9	Upper bearing wedge-shape
1°		554.5		502.2	
2°		399.1		444.9	
3°		245.1	Lower bearing wedge-shape	399.9	Lower bearing wedge-shape

According to Table 3, it can be concluded that under the same combined action of vertical tension and X-direction shear force, the maximum stress of the bearing appears in the case of the upper bearing plate rotation angle of 1°, and the position is the wedge-shaped part of the upper bearing. Under the same combined action of tensile force and the shear force in the Z-direction, the maximum stress of the bearing also appears in the case that the rotation angle of the upper bearing plate is 1°, and the position is the wedge-shaped part of the upper bearing.

Under vertical pressure, the force is mainly exerted by the ball core. Because of the deflection of the upper bearing plate, the contact area between the ball core and the upper bearing plate becomes smaller, so the stress increases. Under the vertical tension, according to the force transmission mechanism of the bearing, the force is mainly exerted by the wedge parts. With the increase of the deflection angle, the stress on the deflection side increases gradually. Under the action of vertical pressure and shear force, the wedge-shaped parts of the upper and lower bearings contact because of the existence of shear force. So the maximum stress does not only appear at the ball core. Under the combined action of vertical tension and shear force, the existence of deflection angle will be adjusted by the ball core, so the maximum stress is less than the undeflection angle.

4. Fatigue life of spherical bearing structure

The finite element stress calculation results obtained by ABAQUS in the previous section were imported into the fatigue software for fatigue life analysis. And the fatigue attributes, algorithm and load of the bearing were set, and then the fatigue calculation results were imported into ABAQUS for post-processing analysis.

4.1. Parameters definition

4.1.1. Fatigue attributes

Correct definition of material fatigue attributes is one of the necessary conditions for fatigue life prediction analysis. The accuracy of material fatigue attributes directly affects the accuracy of fatigue analysis. The model of the spherical bearing is made of cast steel. In order to get accurate fatigue properties, the required materials can be defined in fatigue software. G20Mn5Qt in the material library is selected as the cast steel material, which contains information such as yield strength, ultimate strength, elastic modulus, Poisson's ratio, and the corresponding S-N, ϵ -N curves.

4.1.2. Fatigue algorithm

In the fatigue simulation, it is necessary to choose the appropriate fatigue algorithm. The fatigue algorithms in

the software include biaxial strain fatigue, biaxial stress fatigue, uniaxial fatigue and advanced fatigue. Considering that Brown Miller method in biaxial strain fatigue can obtain relatively accurate results for ductile metals and can provide multi-axis elastoplastic correction when elastic stress is used. Therefore, it is used in this paper to effectively avoid calculation errors.

4.1.3. Fatigue load

When the load input of fatigue analysis is carried out, the node stress results of unit load should be first input, and then it should be taken as the time load history and multiplied by the corresponding load history coefficient. In this paper simulated the fatigue life of the spherical bearing under four working conditions were simulated, namely pressure cyclic load, tension cyclic load, pressure-shear cyclic load, and tension-shear cyclic load. Therefore, when setting the load history coefficient, the selected coefficients are 1, 0 and 1. The load spectrum is shown in Fig. 6.

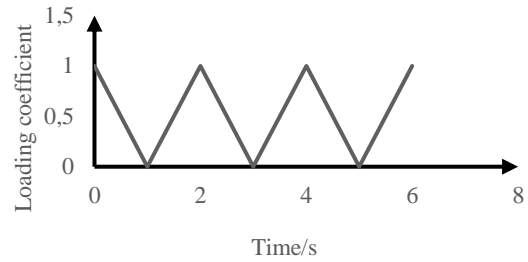


Fig. 6 Load spectrum

4.2. Results and analysis

4.2.1. Vertical pressure action

The stress results of working condition 1 were imported into the software for fatigue life calculation. Taking the rotation angle of 1° as an example, the calculation result is shown in Fig. 7.

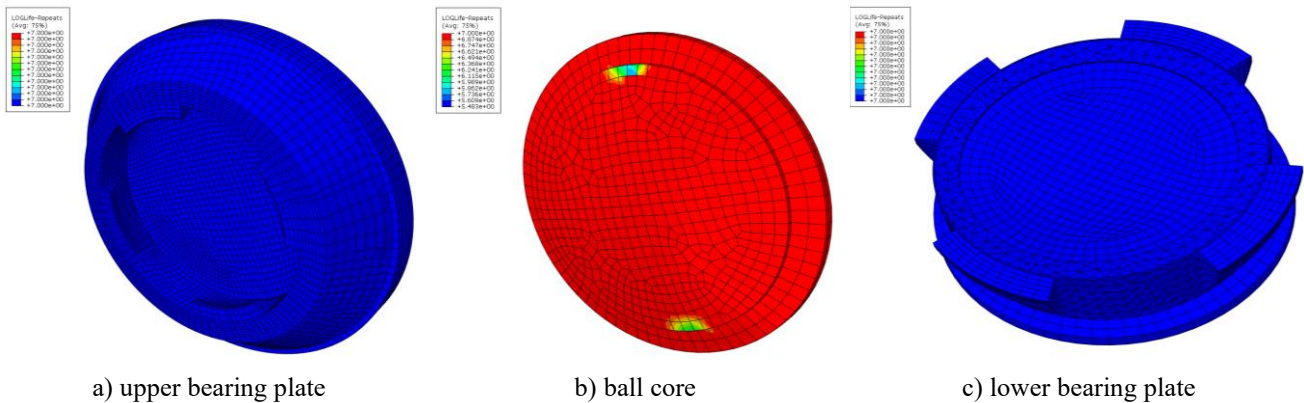


Fig. 7 Fatigue life cloud diagram of the bearing under vertical pressure

As can be seen from Fig. 7, under the action of vertical pressure, when the rotation angle is 1° , the position of the lowest fatigue life of the bearing is the blue position of the ball core, that is, the area where fatigue failure occurs first, which is consistent with the result of the maximum stress calculation. The fatigue life of this position is $10^{5.483}=304088$ times. The fatigue life of the upper bearing plate and the lower bearing plate is close to the "infinite life". The maximum fatigue life limit set for cast steel material is $10E7=10$ million times.

When the upper bearing plate tilt occurs at 0° , 1° , 2° and 3° , the minimum fatigue life is "infinite life", $10^{5.483}=$

304800 times, $10^{5.490}= 309029$ times and $10^{5.488}= 307609$ times, respectively. And the location of the occurrence is at the ball core, which is consistent with the results of the maximum stress position.

4.2.2. Vertical tension action

The stress results of working condition 2 were imported into the software for fatigue life calculation. Taking the rotation angle of 1° as an example, the calculation result is shown in Fig. 8.

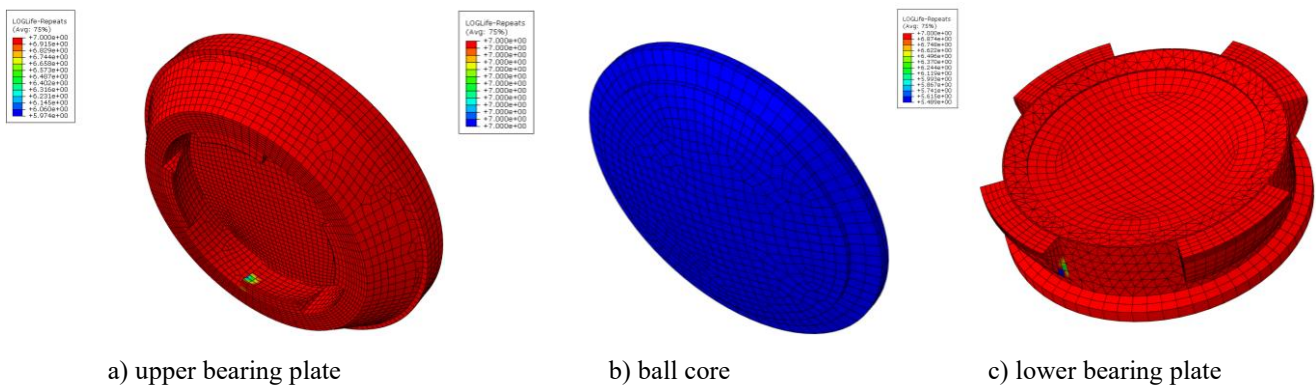


Fig. 8 Fatigue life cloud diagram of the bearing under vertical tension

As can be seen from Fig. 8, under the action of vertical tension, when the rotation angle is 1° , the lowest fatigue life of the bearing is at the wedge-shaped position of the lower bearing plate, which is also the first area where fatigue failure occurs. The fatigue life of this position is $10^{5.489}=308318$ times. The lowest fatigue life of the upper bearing plate is $10^{5.974}=941889$ times, which appears in the wedge-shaped part. Due to the small force on the ball core under the vertical tensile force, the fatigue life of the ball core is close to the "infinite life".

When the upper bearing plate tilt occurs at 0° , 1° , 2° and 3° , the minimum fatigue life is $10^{5.893}=781627$ times,

$10^{5.489}=308318$ times, $10^{5.407}=95940$ times, and "infinite life", respectively. And the location of the occurrence is wedge-shaped region of the lower bearing plate, which is consistent with the results of the maximum stress position.

4.2.3. Combined action of pressure and shear

The stress results of working conditions 3 were imported into the software for fatigue life calculation. Taking the rotation angle of 1° as an example, the calculated results are shown in Figs. 9 and 10.

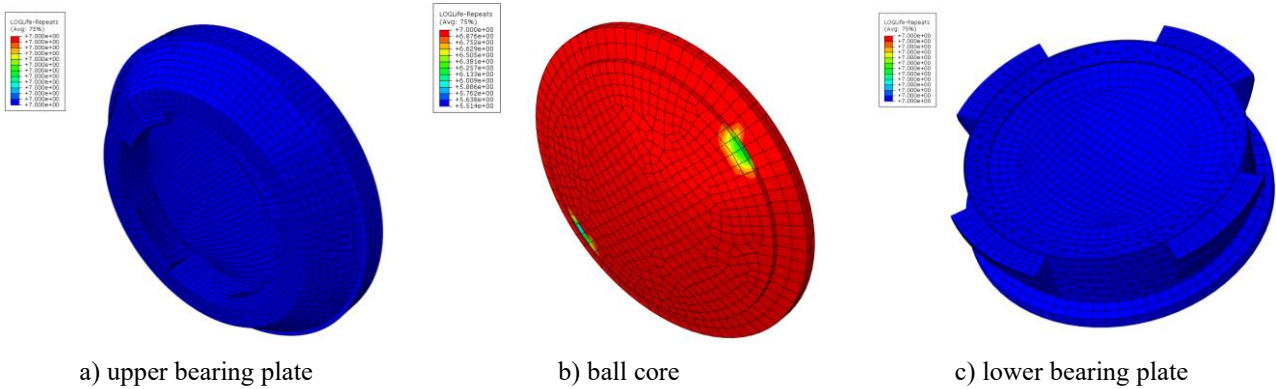


Fig. 9 Fatigue life cloud diagram of the bearing under pressure and X-direction shear force

As can be seen from Fig. 9, under the combined action of vertical pressure and X-direction shear force, when the rotation angle is 1° , the lowest fatigue life of the bearing is at the blue position of the ball core, which is the area where fatigue failure occurs first. The fatigue life of this position is $10^{5.514}=326587$ times. The fatigue life of upper and lower bearing plates is close to "infinite life".

When the upper bearing plate tilt occurs at 0° , 1° , 2° and 3° , the minimum fatigue life is $10^{5.130}=134896$ times, $10^{5.514}=326587$ times, $10^{5.517}=328851$ times and $10^{5.485}=305492$ times, respectively. When the rotation angle is 0° , the first fatigue failure occurs at the wedge-shaped part of the lower bearing plate. At other rotation angles, the first failure occurs at the ball core, which is consistent with the calculation results of the maximum stress.

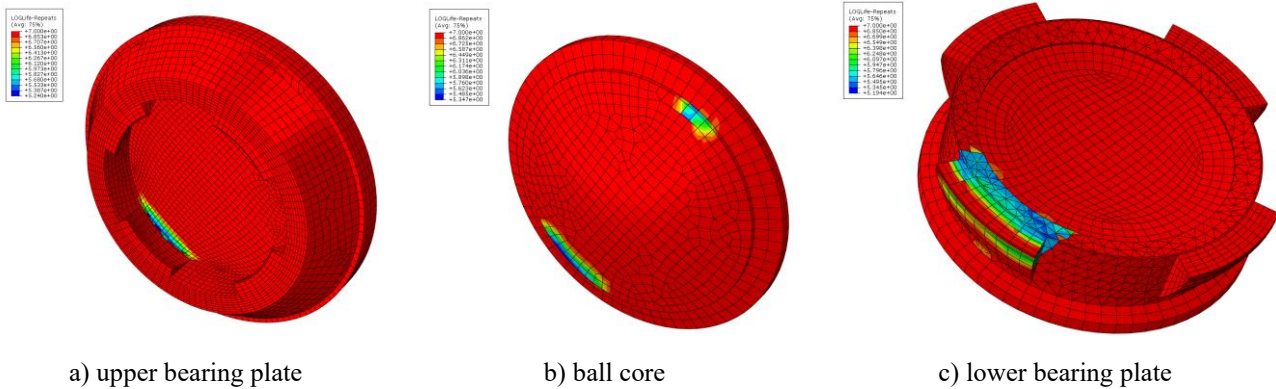


Fig. 10 Fatigue life cloud diagram of the bearing under pressure and Z-direction shear force

According to Fig. 10, under the combined action of vertical pressure and Z-direction shear force, when the rotation angle is 1° , the position of the lowest fatigue life of the bearing is the wedge-shaped part of the lower bearing, and the fatigue life of this part is $10^{5.194}=156314$ times. The minimum fatigue life of the upper bearing plate is $10^{5.240}=173780$ times, which occurs at the root of the wedge-shaped position. The minimum fatigue life of the ball core is $10^{5.347}=222330$ times, which occurs at the part in contact with the lower bearing plate.

When the upper bearing plate tilt occurs at 0° , 1° , 2° and 3° , the minimum fatigue life of the bearing is

$10^{5.235}=171790$ times, $10^{5.194}=156314$ times, $10^{5.183}=152405$ times and $10^{5.231}=170215$ times, respectively. The first place where fatigue failure occurs is the lower bearing wedge-shape, which is consistent with the position of the calculated maximum stress.

4.2.4. Combined action of tension and shear

The stress results after the working condition 4 were imported into the software for fatigue life calculation. Taking the rotation angle of 1° as an example, the calculated results are shown in Fig. 11 and Fig. 12.

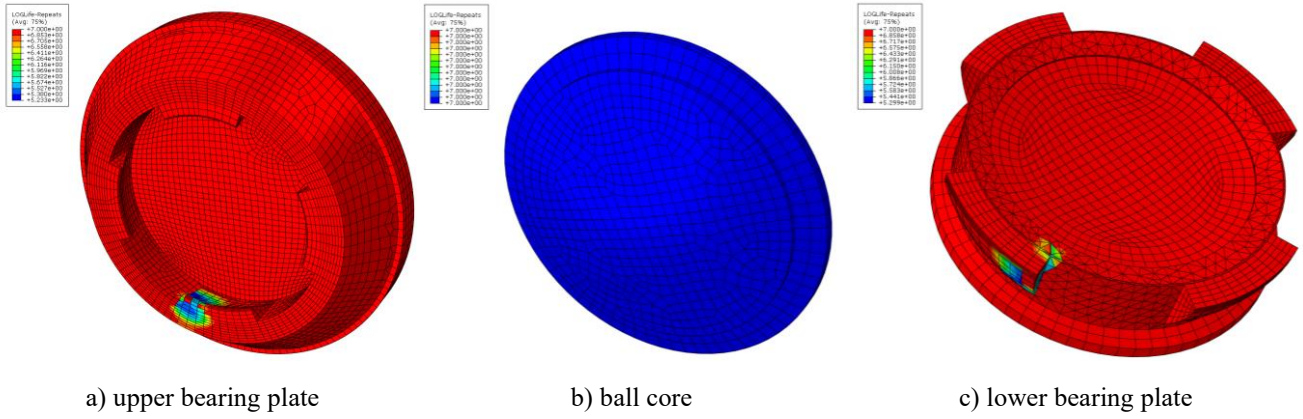


Fig. 11 Fatigue life cloud diagram of the bearing under tension and X-direction shear force

As can be seen from Fig. 11, under the combined action of vertical tension and X-direction shear force, when the rotation angle is 1°, the position of the lowest fatigue life of the bearing is at the wedge-shaped part of the upper bearing plate, which is the area where fatigue failure occurs first. The fatigue life of this position is $10^{5.233}=171001$ times. The minimum fatigue life of the lower bearing plate is $10^{5.299}=199067$ times, which occurs at the wedge-shaped po-

sition. For the ball core, its fatigue life is "infinite life".

When the upper bearing plate respectively occurs 0°, 1°, 2°, 3° tilts, the minimum fatigue life is $10^{5.710}=512861$ times, $10^{5.233}=171001$ times, $10^{6.262}=1836538$ times and "infinite life", respectively. The position occurs at the upper bearing plate wedge-shaped position, the upper bearing plate wedge-shaped position and the lower bearing plate.

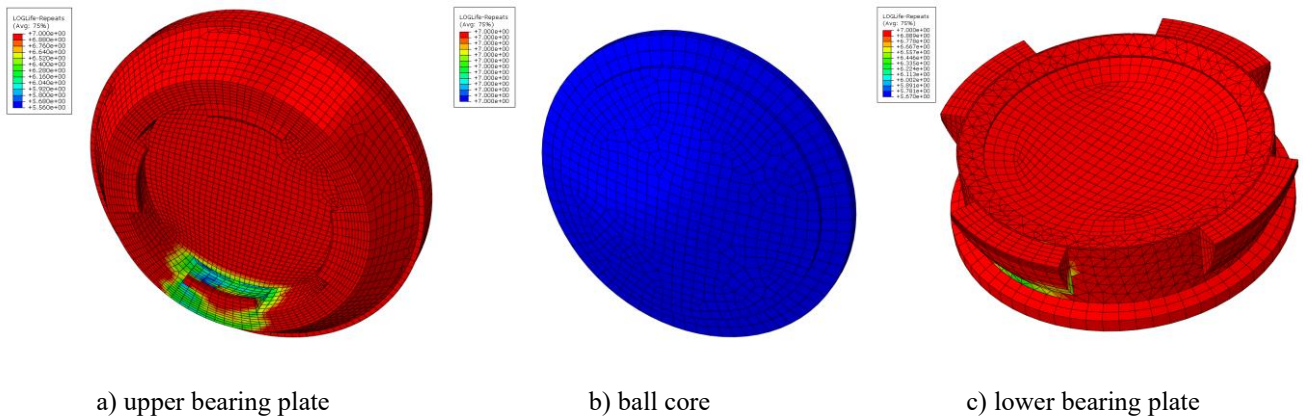


Fig. 12 Fatigue life cloud diagram of the bearing under tensile and Z-direction shear force

According to Fig. 12, under the combined action of vertical tension and Z-direction shear force, when the rotation angle of the upper bearing plate is 1°, the position where the lowest fatigue life of the bearing occurs is the wedge-shaped part of the upper bearing plate, and the fatigue life at this position is $10^{5.560}=363078$ times. The minimum fatigue life of the lower bearing plate is $10^{5.670}=467735$ times, which occurs at the wedge-shaped position corresponding to the upper bearing plate. The fatigue life of the ball core is close to "infinite life" because of the small stress.

When the upper bearing tilts 0°, 1°, 2° and 3°, the minimum fatigue life is $10^{5.778}=599791$, $10^{5.560}=363078$, $10^{5.796}=625172$ and $10^{5.815}=653130$ times, respectively. The location of the occurrence is respectively the upper bearing wedge position, the lower bearing wedge position, the upper bearing wedge position and the lower bearing wedge position.

5. Conclusions

According to this study, the following conclusions can be drawn:

Under vertical pressure load, when the rotation angle of the upper support plate is 1°, the minimum fatigue life of the bearing is the smallest, compared with 1°, when the rotation angle is 2°, 3°, the proportion of the minimum fatigue life increase is 1.4%, 0.9%. When the rotation angle of the upper bearing plate is 0°, the fatigue life is close to the "infinite life".

Under vertical tension load, when the rotation angle of the upper bearing plate is 2°, the minimum fatigue life of the bearing is the smallest. Compared with 2°, when the rotation angle is 0° and 1°, the proportion of the minimum fatigue life increase is 714.7% and 221.3%, respectively. When the rotation angle is 3°, the fatigue life is close to the "infinite life".

Under the vertical pressure and shear force in the X direction, the minimum fatigue life of the upper bearing plate is increased when it is inclined. Compared with 0°, when the inclination angle is 1°, 2° and 3°, the proportion of the minimum life improvement is 142.1%, 143.7% and 126.4%, respectively. Under vertical pressure and shear force in the Z direction, the minimum fatigue life occurs when the rotation angle is 2°, and the minimum fatigue life

increases by 12.7%, 2.5% and 11.6% when the rotation angle is 0°, 1° and 3°, respectively.

Under the vertical tension and shear force in the X direction, when the rotation angle of the upper bearing plate is 1°, the minimum fatigue life of the bearing is the smallest. Compared with 1°, when the tilt Angle is 0° and 2°, the proportion of the minimum fatigue life is 199.9%, 973.9%. When the rotation angle is 3°, the fatigue life is close to the "infinite life". Under the vertical tension and shear force in the Z direction, when the rotation angle of the upper bearing plate is 1°, the minimum fatigue life of the bearing is the smallest. Compared with 1°, when the rotation angle of the upper bearing plate is 0°, 2° and 3°, the proportion of the minimum fatigue life is 65.1%, 72.1% and 79.8%, respectively.

Reference

1. **Fan, Z.; Yang, S.; Luan, H.Q.** 2011. Research progress and practice of spatial structure joint design, *Journal of Building Structures* 32(12):115.
<http://dx.doi.org/10.14006/j.jzjgxb.2011.12.003>.
2. **Chen, Z. H.; Wu, F.; Yan, X. Y.** 2007. A review of domestic spatial structure nodes, *Building Science* (09):93-97.
<http://dx.doi.org/10.3969/j.issn.1002-8528.2007.09.024>.
3. **He, W.** 2011. Analysis of Bridge Bearing Structure and Research on Fatigue Performance. Southwest Jiaotong University, China.
<http://dx.doi.org/10.7666/d.y2108823>.
4. **Nie, Y. T.; Li, Y. M.** 2014. Influence Analysis of Boundary Condition on Stability of Reticulated Shell Structure. *Shanxi Architecture*, 40(03):68-69.
<http://dx.doi.org/10.13719/j.cnki.cn14-1279/tu.2014.03.035>.
5. **Li, J.** 2006. Structural Design of Super Large Tonnage Spherical Bearing. Chongqing: Chongqing University
6. **Fu, G.; Luo, Y. Z.; Lai, D. D.** 2002. Experimental study on polytetrafluoroethylene (PTFE) lattice bearing, *Proceedings of the 10th academic conference on spatial structure*. Beijing, China.
7. **Peng, T. B.; Li, J. Z.; Fan, L. C.** 2007. Development and Application of Hyperboloid Spherical Bearing, *Journal of Tongji University: Natural Science* 35 (2): 176-180.
<http://dx.doi.org/10.3321/j.issn:0253-374X.2007.02.007>.
8. **Zang, X. Q.** 2009. Design of large tonnage and large displacement spherical bearing, *Railway Construction* (04): 1-3
<http://dx.doi.org/10.3969/j.issn.1003-1995.2009.04.001>.
9. **Shao, X. D.** 2002. *Bridge Engineering*. 1st Ed. Wuhan University of Technology Press.
10. **Wang, L. Q.; Xu, G. B.** 2002. Application of damping double curve steel bearing in space structure, *Steel Structure* 17(5): 32-34.
<http://dx.doi.org/10.3969/j.issn.1007-9963.2002.05.012>.
11. **Cui, L.; Xu, G. B.** 2000. Development of Universal Bearing, Universal Rotation, Seismic and Vibration Absorbing Spheres Bearing: *Proceedings of the Ninth Conference on Space Structures*, Xiaoshan, China.
12. **Dexter, E. M.; Lee, M. M. K.** 1999. Static strength of axially loaded tubular K-joints, *Journal of Structural Engineering* 125(2).
[http://dx.doi.org/10.1061/\(ASCE\)0733-9445\(1999\)125:2\(194\)](http://dx.doi.org/10.1061/(ASCE)0733-9445(1999)125:2(194)).
13. **Kuang, J. G.; Potrin, A. B.; Leick, R. D.** 1977. Stress concentration in tubular joint, *Offshore Technology Conference*, Houston, Texas.
<http://dx.doi.org/10.2118/5472-PA>.
14. **Zhao, H. L.; Ma, J. A.** 1992. Study of the behavior of joints, *Space Structure*.
15. **Shen, Y. L.; Fan, Z.; Zhang, P. J.** 2011. Design and analysis of spherical bearing for building structure, *Steel Structure* 26(06): 6-11.
<http://dx.doi.org/10.3969/j.issn.1007-9963.2011.06.002>.
16. **Shi, W. X.; Liu, K. Y.; Wang, L. Z.** 2009. Shaking table test study on damping performance of steel bearing with net frame shock absorber ball, *Northwest Seismological Journal* 21(4): 344-348.
<http://dx.doi.org/10.3969/j.issn.1000-0844.2009.04.006>.
17. **He, W.; Wang, S. H.; Wang, G. C.** 2012. Research on the structure and performance of spherical bearing, *Railway Construction* (5):14-17.
<http://dx.doi.org/10.3969/j.issn.1003-1995.2012.05.005>.
18. **Wu, W. Z.; Li, H. W.; Song, X. Y.** 2020. Ultra-low cycle fatigue failure characteristics of anchor bolt in bolted ball bearing joints, *Science Technology and Engineering* 20(15): 6182-6190.
<http://dx.doi.org/10.3969/j.issn.1671-1815.2020.15.042>.
19. **Liu, J. M.** 2011. Fatigue test research on light rail bearing of chongqing caiyuanba yangtze river bridge, *Chongqing Jiaotong University*.
<http://dx.doi.org/10.7666/d.y1902351>.
20. **He, W. F.; Zhou, L. B.; Xu, H.; Liu, W. G.** 2019. Takeshi Sanshan. Fatigue temperature mechanics test of lrb bearing and influence analysis of seismic response of isolated structure, *Journal of Vibration Engineering* 32(02): 314-323.
<http://dx.doi.org/10.16385/j.cnki.issn.1004-4523.2019.02.015>.
21. **Tie, M. L.** 2010. Research on the Life of Bridge Extensible Device and Bearing. Chang 'an University.
<http://dx.doi.org/10.7666/d.y1729135>.
22. **Wang, L.; Li, H. W.; Song X. Y.; Wang, X. Y.; Li, Y. Y.** 2020. *Science Technology and Engineering* 20(24): 9996-10002.
<http://dx.doi.org/10.3969/j.issn.1671-1815.2020.24.045>.
23. **Wang, Q.; Li, H. W.; Song, X. Y.; Wang, X. Y.** 2020. Experimental study on damage accumulation of anchor bolt in ultra-low cycle fatigue test of transition plate bearing joints, *Science Technology and Engineering* 20(20): 8325-8330.
24. **Wang, J.** 2007. Finite element analysis and experimental study on spherical bearing considering contact surface characteristics, *Tongji University*.
<http://dx.doi.org/10.7666/d.y1031832>.
25. Ministry of Housing and Urban-Rural Development, 2016. PRC.GB50011-2010 Code for Seismic Design of Buildings. Beijing: China Building and Building Press.
26. Ministry of Housing and Urban-Rural Development, 2018. PRC.GB50017-2017 Steel Structure Design Standard. Beijing: China Building and Building Press
27. China Engineering Construction Standardization Association. 2008. CECS 235:2008 Technical Specification for Application of Cast Steel Joints. Beijing: China Planning Press.

28. Ministry of Housing and Urban-Rural Development, PRC. 2017. Spherical bearing of building steel structure.
29. **Huang, Q. W.** 2018. Study on constitutive model of cast steel considering cumulative damage effect, Tianjin University.
30. **Liu, M. S.; Li, J. Y.; Chen, L. X.** 2019. On the response and prediction of multi-layered flexible riser under combined load conditions, *Engineering Computations* 8(36): 2507-2529.
<https://doi.org/10.1108/EC-10-2018-0493>.

Y. Fu, H. Wang, Y. Fu

STUDY ON THE FATIGUE OF A SPHERICAL BEARING UNDER DIFFERENT LOADING CONDITIONS CONSIDERING ROTATION EFFECT

S u m m a r y

In order to study the fatigue life of a large spherical bearing under actual working conditions, the finite element software ABAQUS was firstly used to establish the spherical bearing model and simulate the mechanical properties of the bearing at different rotation angles under four working conditions of pressure, tension, pressure shear, and tension shear. And the stress characteristics under the corresponding working conditions were obtained. On this basis, the stress results were imported into the fatigue analysis software, and

the fatigue life of each component of the spherical bearing was calculated under the four working conditions. The results show that: the rotation angle of the upper bearing plate has obvious influence on the maximum stress of the bearing under various working conditions. The maximum stress is 554.5 MPa and locates in the wedge-shaped region of the lower bearing plate under the working condition of the joint action of tension and X-direction shear force, and when the rotation angle of the upper bearing plate is 1° . In other working conditions, the maximum stress of the bearing mostly occurs in the wedge-shaped position of the upper and lower bearing plates. The influence of the rotation angle of the upper bearing plate on the minimum fatigue life of the bearing shows the same trend as the influence on the maximum stress. The minimum fatigue life is 13,000 times and locates in the wedge-shaped region of the lower bearing plate under the working condition of the joint action of tension and X-direction shear force, and when the rotation angle of the upper bearing plate is 1° . In other working conditions, the lowest fatigue life of the bearing is also mostly found in the wedge-shaped area of the upper and lower bearing plates. So, the wedge-shaped area should be strengthened in the design.

Keywords: spherical bearing, finite element analysis, static performance, fatigue life.

Received November 05, 2021

Accepted June 14, 2022



This article is an Open Access article distributed under the terms and conditions of the Creative Commons Attribution 4.0 (CC BY 4.0) License (<http://creativecommons.org/licenses/by/4.0/>).